ELSEVIER

Journal of Power Sources 74 (1998) 155–157

JOURNAL OF POWER SOURCES

Study of early cycling deterioration of a Ni/MH battery by electrochemical impedance spectroscopy

Shaoan Cheng *, Jianqing Zhang, Hong Liu, Yongjun Leng, Anbao Yuan, Chunan Cao

Department of Chemistry, Zhehiang University, Hangzhou, 310027, China

Received 28 January 1998; accepted 8 February 1998

Abstract

a.c. impedance measurements are made on spiral-wound, size 4/5A, Ni/MH batteries, which are prepared by using direct-seal technology. Both the positive and the negative electrodes are fabricated by filling in a porous nickel substrate with the active materials. The main purpose of the investigation is to determine the cause(s) of the early cycling deterioration of this foam-type battery. The results demonstrate that the cycle-life curve can be divided into three parts. After little change in capacity and voltage, deterioration of the Ni/MH battery occurs as the voltage performance decreases. This is followed by a sharp decrease in both the discharge capacity and the voltage performance. The decrease in voltage performance is due to drying of the separator, which increases the total ohmic resistance of the battery, while the decrease of discharge capacity is due to an inactive surface that increases the charge-transfer resistance of the battery.

Keywords: Nickel/metal hydride battery; Impedance; Foam nickel; Capacity; Voltage performance

1. Introduction

Electrochemical impedance spectroscopy (EIS) has many advantages, such as applying small amplitude a.c. signals to systems composed of a wide range of materials and providing detailed information on the sub-process of the system. EIS is particularly suitable for studying the reaction kinetics of electrodes and batteries. Many impedance studies have been carried out on lead/acid [1–3], Ni/Cd [4–6], Zn/MnO_2 [7], Na/S [8], and Ni/H_2 [6] batteries.

Only a few previous EIS studies on metal hydride electrodes and Ni/MH batteries have been reported. Kuriyama et al. [9] used EIS to study the degradation mechanism of metal hydride electrodes and the activity of the alloy, and found that the kinetics of the electrochemical hydriding/dehydriding reaction of an alloy electrode depends upon the reaction resistance on the alloy surface. Zhang et al. [10] developed a mathematical model to study the mechanism of the hydriding/dehydriding reaction, and the effect of the structure and the composition of the MH electrode in order to enhance the performance of such electrodes. These studies focused mainly on the effect of state-of-charge on the impedance of the battery. Several investigators have studied battery degradation with EIS. Reid [6] applied EIS to investigate Ni/Cd and Ni/H_2 lightweight batteries. It was found that the battery case could be used as a reference electrode for Ni/Cd batteries, and that EIS measurements could be used to determine which electrode is responsible for the loss of performance. A parallel circuit of a charge-transfer resistance and a constant-phase element in series with the ohmic resistance was found to fit the data well. After this, Reid [11] measured the impedance of a spiral-wound nickel/metal hydride battery cycled in a simulated low earth orbit. He found that the impedance changed only slightly over the course of 2000 LEOs (low earth orbit regimes) at 50% depth-of-discharge (DoD) with approximately 5% overcharge. Both the nickel electrode and the metal hydride electrode apparently contribute to the impedance of the battery, with the larger portion probably due to the nickel electrode. Haak [12] found that a rapidly increasing value of the low-frequency slope in the Nyquist plot for a Ni/Cd battery was indicative of potential battery failure.

In the present study, the impedance of a foam-type Ni/MH battery is measured with charge/discharge cycling in order to determine the main causes of early cycling deterioration.

* Corresponding author.

0378-7753/98/$19.00

2. Experimental

Spiral-wound, size 4/5A, Ni/MH batteries were prepared by using direct-seal technology. A non-sinter nickel positive electrode was fabricated by applying a paste, which was a mixture of nickel hydroxide powder and water with a binding medium, onto a foam–nickel substrate. Metal hydride electrodes were made by mixing $MINi_{3.45}(Co,Mn,Ti)_{1.55}$ hydrogen storage alloys and acetylene black with a binding medium to form a paste, applying the paste to the foam–nickel matrix, drying, and rolling. The separator was non-woven polypropylene. The alkali electrolyte was a mixture of KOH and LiOH. The design capacity of battery was 1.5 A h.

The batteries were first activated by charging at the $0.1C$ rate for 15 h and discharging at $0.2C$ using a cut-off voltage of 1 V. The batteries were then charged at the $0.2C$ rate for 6.5 h and discharged at $0.2C$ 1 V (C is the nominal capacity of the battery). This process was repeated four times. After this, the cycle-life test of the battery was conducted under the following conditions: charge at 850 mA for 2.2 h using a ΔV of 10 mV; discharge at 500 mA using a cut-off voltage of 0.9 V.

Impedance measurements were made by means of a Solartron 1250 Frequency Response Analyzer in conjunction with a Solartron 1287 Electrochemical Interface. Measurements were made at the given cycle, in which case the state-of-charge of the battery was 20%. The positive electrode was studied, and the negative electrode as the counter electrode and the reference electrode. The voltage perturbation used in the present work was 10 mV. Impedance was measured from 10 kHz to about 1 mHz.

3. Results and discussion

Both the positive electrode and the negative electrode apparently contribute to the impedance of the battery. A typical Nyquist plot is shown in Fig. 1. At high frequencies, the plot starts as a semicircle, and as the frequency decreases, it changes to a straight line. The model for the essential features of battery is represented by the electrical equivalent circuit shown in Fig. 2, where: R_s is the total ohmic resistance of the solution and the separator as well as the electrodes; R_t is the charge-transfer resistance of the electrodes; Z_w is the Warburg impedance; Q_c is the constant-phase element in order to consider semicircles with a depressed shape.

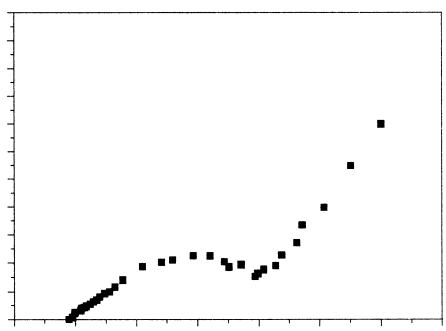

Fig. 1. Typical Nyquist plot of battery.

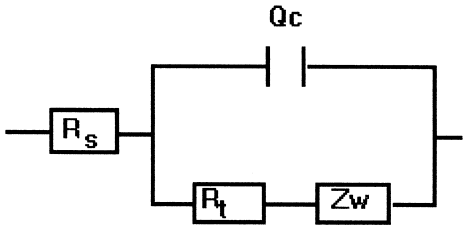

Fig. 2. Equivalent circuit for battery.

The decay of the total discharge capacity and voltage characteristic (discharge capacity over 1.2 V) of the battery with cycle number is shown in Fig. 3. The cycle–life curve can be divided into three parts. In the first part (characteristic point A), the voltage characteristic and the total discharge capacity of the battery are essentially constant. In the second part (characteristic point B), the voltage characteristic decays, but the total discharge capacity stays constant. In the third part (characteristic C), both the

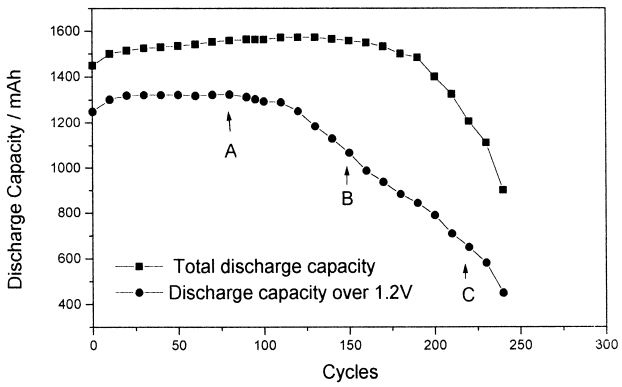

Fig. 3. Total discharge capacity and voltage characteristic (discharge capacity over 1.2 V) vs. number of cycles.

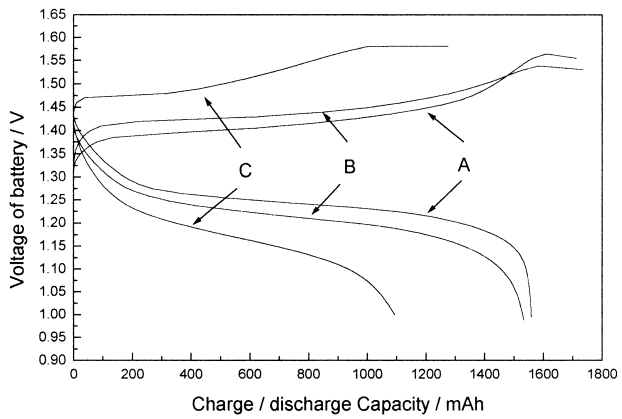

Fig. 4. Charge–discharge curves of battery at points A, B and C.

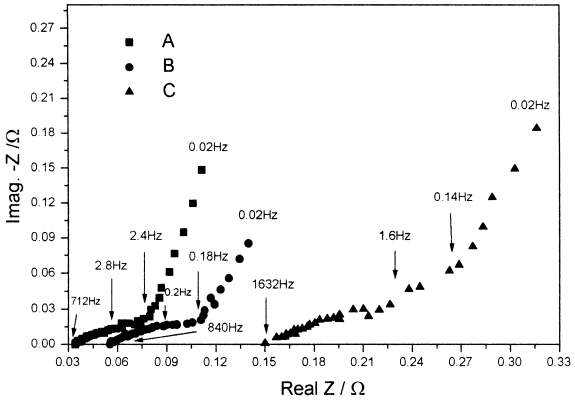

Fig. 5. EIS of battery measured at points A, B and C.

voltage characteristic and the total discharge capacity decrease rapidly. The charge–discharge curves of the battery at points A, B and C are shown in Fig. 4.

The EIS of the battery at points A, B and C are presented in Fig. 5. The data were fitted using the equivalent circuit shown in Fig. 2 with the ohmic resistance in series with a parallel combination of a constant-phase element, and a resistor representing the kinetic resistance. It is found that the ohmic resistance (R_s) remains virtually constant during the first part of cycling, increases in the second stage, and increases steeply in the third stage. The charge-transfer resistance (R_t) decreases slightly during the first stage, stays essentially constant in the second stage, and increases rapidly in the third stage. The impedance parameters at points A, B and C are listed in Table 1. It can be seen that, with cycling, the Warburg resistance, Z_w, caused by the diffusion process, increases but the capacitance, which provides interface information, decreases. Batteries cycled to points A, B and C were dissected and recycled in a glass cup that contained the electrolyte under the following conditions: charge at 850 mA for 2 h; discharge at 500 mA, 1.0 V cut-off. It was found that the total discharge capacity and voltage characteristic of the batteries at points A and B were always the same as those for the initial stage of cycling. The total discharge capacity and voltage characteristic of the battery at point C is greatly decreased, compared with those for the initial stage of cycling. It is also found that the polarization of negative electrode at point C was increased markedly.

These data indicate that the decrease in the voltage characteristic of the battery is due to drying out of the separator that increases the R_s of the battery, and that decay of the total discharge capacity is due to an inactive surface that increases the R_t of the battery.

Table 1
Impedance parameters

	R_s (Ω)	R_t (Ω)	Z_w (Ω)	Q_c^a
A	0.036	0.0824	0.0435	9.8
B	0.053	0.0830	0.0466	8.5
C	0.152	0.114	0.0557	6.7

[a]The unit of Q_c is F^N; F is the Faraday constant; N is the dispersion coefficient.

4. Conclusions

The early cycling deterioration of a Ni/MH battery appears first as the voltage performance decreases. It is then followed by a sharp decrease of discharge capacity and voltage performance. The decline in voltage performance is due to drying out of the separator, which increases the R_s of the battery, while the decrease in the discharge capacity is due to an inactive surface that increases the R_t of the battery.

Acknowledgements

The authors are grateful to the Zhejiang provincial Natural Science Foundation of China and Chinese ‘863’ Project for support of this work.

References

[1] M.L. Gopikanth, S. Sathyanarayana, J. Appl. Electrochem. 9 (1979) 369.
[2] V.V. Viswanathan, A.J. Salkind, J.J. Kelley, J.B. Ockerman, J. Appl. Electrochem. 25 (1995) 729.
[3] P.R. Roberge, E. Halliop, G. Verville, J. Smit, J. Power Sources 32 (1990) 262.
[4] V.V. Viswanathan, A.J. Salkind, J.J. Kelley, J.B. Ockerman, J. Appl. Electrochem. 25 (1995) 716.
[5] A.H. Zimmerman, M.R. Martinelli, M.C. Janecki, C.C. Badcock, J. Electrochem. Soc. 129 (1982) 289.
[6] M.A. Reid, J. Power Sources 29 (1990) 467.
[7] S.A.G.R. Karunathilaka, N.A. Hampson, R. Leek, T.J. Sinclair, J. Appl. Electrochem. 11 (1981) 365.
[8] P.J. Johnson, A.A. Koenig, J. Electrochem. Soc. 137 (1990) 1121.
[9] N. Kuriyama, T. Sakai, H. Miyamura, I. Uechara, H. Ishikawa, J. Electrochem. Soc. 139 (1992) L73.
[10] W.L. Zhang, M.P.S. Kumar, J. Electrochem. Soc. 142 (1995) 2935.
[11] M.A. Reid, J. Power Sources 47 (1994) 277.
[12] R. Haak, C. Ogden, D. Tench, S. Di Stefano, J. Power Sources 12 (1984) 289.